

## **INTERFACIAL FRACTURE TOUGHNESS OF CONCRETE REPAIR MATERIALS**

V. C. Li, Y. M. Lim, and D. J. Foremsky  
Advanced Civil Engineering Material Research Laboratory  
Department of Civil and Environmental Engineering  
The University of Michigan, Ann Arbor, U.S.A.

### **Abstract**

Application of any repair material results in bimaterial interface between the repair material and the existing material of the repaired structure. Due to defects on the interface, and shrinkage and/or thermal loading, interface failure can limit the performance of the repaired system. Such failure can take the form of delamination or spalling of the repair material. Several tests are currently used to quantify the performance of concrete repair material, all of which define the tensile or shear bond strength of the interface. These tests cannot be expected to have predictive capability in durability of repair systems in the field. Recent development of the theory of interface fracture in bimaterial interfaces suggests techniques for proper characterization of interface properties in repair systems.

In this paper, experimental results of interface toughness of substrate concrete with several repair materials are reported. Interfacial fracture toughness is presented as a function of load mixity -- a ratio of opening versus shear mode of loading. Repair materials studied include ordinary concrete, fiber reinforced concrete, and a quick-setting highway patch material.

## 1 Background

As infrastructure around the world ages, the rehabilitation of existing structures to extend the service life of the facilities becomes more important (Mailvaganam, 1992; Allen et al, 1993). Many repair materials and techniques have been specifically developed for concrete repair aimed at providing strong, longer-lasting repair at low cost. Even with evolving innovative materials and techniques, many outstanding repair problems remain (Warner, 1994). In many cases, the repaired structure still fails in the repair part, around the repair part, or at the interface between newly applied and existing material (Emmons, 1994). In particular, failure as a result of cracks initiated at the interface could be found in many repaired structures.

Application of any repair materials results in bimaterial interfaces between the newly applied material and the base concrete. The performance of the repaired system is directly related to the properties of such interfaces. For example, the debonding failure of interface leads to the deficiency of the section modulus of a repaired structure such as bonded overlay on old bridge decks or pavement systems (Calvo, 1991; Jonston et al., 1989). In addition, interface failure often leads to surface delamination or/and spalling resulting in a reduction in the service life of the repaired structure. Therefore, the performance of interface in a repair system is one of the most important factors for durability of repaired concrete structures. Well-designed repair system can significantly reduce maintenance cost.

To quantify the performance of interfaces, several standardized bond strength tests (ASTM C496, ASTM C882, ASTM E149, and RILEM 13R etc.) are currently used in practice, all of which define the tensile or shear strength of the interface (Emmons, 1994). These tests may be useful for ranking of repair materials, but are not expected to have predictive capability. In situ, many defects can form during repair procedures, providing stress concentration at the tip of the crack-like defects. Failure initiated by fracture propagation from these defects in brittle concrete can be expected to be governed by fracture toughness rather than tensile or compressive strength. This behavior is analogous to the fracture behavior in monolithic concrete structures, which has been extensively studied theoretically and experimentally in the last two decades (e.g. Elfgren, 1989). Therefore, determining the integrity of a concrete repair system requires, among other things, the experimental determination of interface toughness based on interface fracture mechanics (He et al., 1991).

Interface fracture mechanics can serve as an analytic tool to predict the conditions under which an interface crack will propagate in-plane, and when it will kink-out from the interface as well as the

load magnitude necessary to drive the crack. To utilize this interface fracture mechanics concept, interface toughness has to be experimentally determined. The main objective of this paper is to report on an experimental technique for characterization of interface toughness between old concrete and new repair material. Preliminary toughness data on several repair material/concrete systems are also reported. In the following section, the basic concept of interface fracture mechanics relevant to interface toughness characterization will be summarized (He et al., 1989; Hutchinson et al., 1991; Malyshev et al., 1965).

A final goal of this research is the development of repair materials highly resistant to delamination and spalling failure, based on the understanding of interface cracking behavior. The idea is to engineer the microstructure of the repair material in order to resist interfacial fractures. This research should lead to a more systematic materials engineering methodology aimed at enhancing the life-time of repaired concrete structures.

## 2 Interface fracture toughness

In many cases, problems in repaired structures relate to cracking along the interface or kinking of cracks out of the interface. In the interface cracking case, the bimaterial interface is relatively "weaker" than the bordering materials, meaning that the interface crack will propagate exclusively along the least resistance path, interface. In the crack kinking case, the interface is relatively "tougher" than at least one of the other parts of the adjoining materials. Quantitative evaluation of whether an interface crack will advance straight ahead or kink-out of the interface into the repair material requires interfacial fracture toughness to be measured. Even when the interface crack stays in-plane, a mixed mode loading results. Fracture mechanics of homogeneous material cannot explain this behavior. In this section, interface fracture mechanics will be briefly reviewed with special focus on its application to interface toughness measurement. A comprehensive review of interface fracture mechanics can be found in Hutchinson and Suo (1991).

Assume two isotropic elastic materials joined along the x-axis as illustrated in Fig. 1 with material 1 above the interface and material 2 below. Here,  $\mu_i$ ,  $E_i$  and  $\nu_i$  are the shear modulus, the Young's modulus, and the Poisson's ratio of the respective materials ( $i=1,2$ ).

The Dundurs' elastic mismatch parameters for bimaterial, reinterpreted by Hutchinson and Suo (1991), are defined as

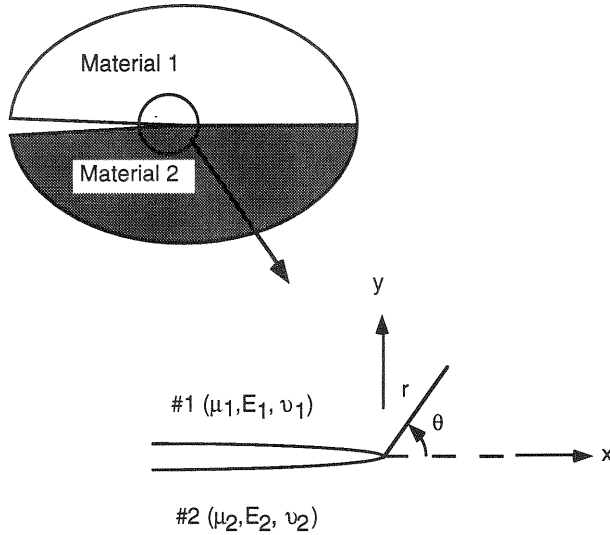


Fig. 1. Geometry of interface crack

$$\alpha = \frac{\bar{E}_1 - \bar{E}_2}{\bar{E}_1 + \bar{E}_2}, \text{ and } \beta = \frac{1}{2} \frac{\mu_1(1-2\nu_2) - \mu_2(1-2\nu_1)}{\mu_1(1-\nu_2) + \mu_2(1-\nu_1)}. \quad (1)$$

$\bar{E}_i \equiv E_i / (1 - \nu_i^2)$  for plane strain and  $\bar{E}_i \equiv E_i$  for plane stress. Physically,  $\alpha$  measures the magnitude of mismatch of the elastic tensile moduli of the bimaterial. For material 1 much stiffer than material 2 ( $E_1 \gg E_2$ ),  $\alpha$  approaches +1. For material 2 much stiffer than material 1 ( $E_2 \gg E_1$ ),  $\alpha$  approaches -1. When there is no mismatch ( $E_1 = E_2$ ),  $\alpha$  is equal to 0. The parameter  $\beta$  measures the mismatch in the in-plane bulk modulus. Again,  $\beta = 0$  when there is no moduli mismatch or when both materials are incompressible ( $\nu_i = 0.5$ ). In plane strain,  $\beta$  equals  $3/8 \alpha$  when  $\nu_1 = \nu_2 = 0.2$  appropriate for most cementitious materials.

Interface crack problems were investigated by Cherepanov (1962), England (1965), Erdogan (1965), and Rice and Sih (1965). The crack tip stress field (Rice, 1988) for plane problems can be written as

$$\sigma_{jk} = \text{Re}[Kr^{i\epsilon}](2\pi r)^{-1/2} \tilde{\sigma}_{jk}^I(\theta, \epsilon) + \text{Im}[Kr^{i\epsilon}](2\pi r)^{-1/2} \tilde{\sigma}_{jk}^{II}(\theta, \epsilon) \quad (2)$$

where  $i = \sqrt{-1}$ ,  $\tilde{\sigma}_{jk}^I(\theta, \epsilon)$  and  $\tilde{\sigma}_{jk}^{II}(\theta, \epsilon)$  are dimensionless angular functions. Other notations are defined in Fig. 1. Also,

$$\varepsilon \equiv \frac{1}{2\pi} \ln \left( \frac{1-\beta}{1+\beta} \right). \quad (3)$$

The complex interface stress intensity factor ( $K = K_1 + iK_2$ ) can be expressed using real and imaginary parts  $K_1$  and  $K_2$ . The complex stress intensity factor for any plane elasticity interface crack problem can be written in the general form

$$K = K_1 + iK_2 = (\text{applied stress}) \times FL^{1/2-i\varepsilon}. \quad (4)$$

Here  $L$  is an in-plane length, and  $F$  is a complex dimensionless function containing material and geometric information.

The energy release rate  $G$  for interface crack in-plane advance can be related (Malyshev et al., 1965) to  $K_1$  and  $K_2$  via the stress field described in Eqn (2) and the corresponding displacement field on the crack line (Rice, 1988):

$$G = \frac{(1-\beta^2)}{E_*} (K_1^2 + K_2^2) = \frac{(1-\beta^2)}{E_*} |K|^2 \quad (5)$$

where,

$$\frac{1}{E_*} = \frac{1}{2} \left( \frac{1}{E_1} + \frac{1}{E_2} \right). \quad (6)$$

Thus, the energy release rate for interface crack is a function of mode mixity. For simple notation, the mode mixity  $\hat{\psi}$  can be defined using phase angle at a distance  $l$  from crack tip with use of Eqn (2).

$$\hat{\psi} = \tan^{-1} \left[ \text{Im}(Kl^{i\varepsilon}) / \text{Re}(Kl^{i\varepsilon}) \right] = \tan^{-1} \left[ (\sigma_{12} / \sigma_{22})_{r=l} \right] \quad (7.a)$$

For the special case when  $\beta = \varepsilon = 0$ ,

$$\hat{\psi} = \tan^{-1} (K_2 / K_1) \equiv \psi \quad (7.b)$$

The relation between  $\hat{\psi}$  and  $\psi$  can be expressed as

$$\hat{\psi} = \psi + \varepsilon \ln(l / L) \quad (8)$$

The choice of reference length  $l$  is somewhat arbitrary (Rice, 1988). However,  $r = l$  should define a material point within the  $K$ -dominant zone.

The interface crack will start to propagate along the interface when the driving force  $G$  is equal to the interface toughness  $\Gamma(\hat{\psi})$ .

$$G = \Gamma(\hat{\psi}) \quad (9)$$

The dependence of  $\Gamma$  on  $\hat{\psi}$  has been known for the interface of a number of non-cementitious bimaterial systems (Wang et al., 1990; Liechti et al., 1991; O'Dowd et al., 1992b), and for aggregate-mortar interface (Buyukozturk, 1993).

### 3 Experimental program and results

#### 3.1 Set-up of interface toughness test

Many different set-ups have been developed to measure interface toughness at different phase angles (Cao et al., 1989; Charalambides et al., 1989; Wang et al., 1990). In this study, the symmetric and asymmetric four point bending set-up shown in Fig. 2 is selected. The reasons why this set-up is selected are (i) the calibration functions have already been developed, (ii) the set-up affords a large range of phase angles with only a single specimen geometry, and (iii) this set-up is relatively easy to handle and test.

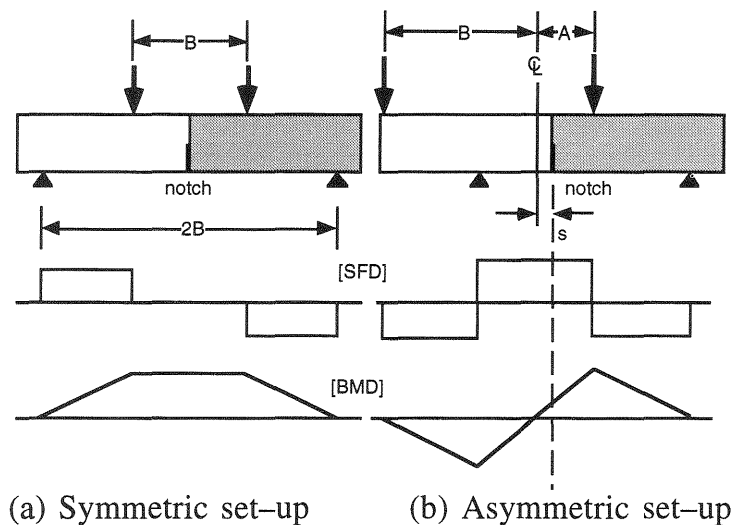


Fig. 2. Set-ups and loading conditions

Fig. 2 schematically shows the loading arrangement, and the variation of the shear force (SFD) and bending moment (BMD) along the length of the specimen. The symmetric set-up in Fig. 2(a) is used for approximately zero degree phase angle (exactly zero for  $\varepsilon = 0$ ). The asymmetric set-up in Fig. 2(b) is used for varied phase angle with different offset  $s$ . The offset is measured from the center of loading line (zero moment) to the interface. If the offset  $s$  equals zero, the phase angle is approximately  $90^\circ$  (exactly  $90^\circ$ , pure shear stress, for  $\varepsilon = 0$ ). The larger offset corresponds to the smaller phase angle. When the offset is 45, 20 and 12 mm, the phase angle is about  $15^\circ$ ,  $30^\circ$  and  $45^\circ$ , respectively.

Total beam length, beam depth ( $W$ ), beam thickness ( $t$ ), and notch length ( $a$ ) are 45.72 cm, 7.62 cm, 3.81 cm, and 3.05 cm (18 in., 3 in., 1.5 in., and 1.2 in.), respectively. The notch on the interface locates at the middle of the specimens between two equal lengths of two different materials. For a toughness test, notch to beam depth ratio is usually varied from 0.4 to 0.5. In this interface toughness test, 0.4 for notch/beam depth ratio is selected. The  $A$  and  $B$  chosen to correspond to the capability of loading fixture are 7.62 cm and 15.24 cm, respectively.

The base material was cast in the left half side of mold, in the same mold in which the complete bimaterial beam was later cast. The repair material was cast into the right hand side of mold with the base material placed back in the left hand side of the mold after five weeks of curing. Before the repair material was cast, the interface surface in the base material was ground using a bench grinder to remove contamination from demolding oil and surface layer of concrete. The condition of interface surface greatly influences the interface toughness. Rougher surface can provide higher interface toughness especially at higher phase angle. So, uniformity among specimens is important, and almost same interface roughness condition is attempted. Such smooth grinding surface is expected to provide a lower bound of the interface toughness when compared with natural interfaces created in field repair systems.

### 3.2 Measurement and calibration

The specimens are tested under displacement control (at a rate 0.005 mm/sec.) in a closed-loop MTS loading frame with a capacity of 25 kips. The displacement of the loading head and loads from load cell are continuously recorded during the test.

The calibration for this interface specimen was developed based on finite element analysis assuming linear elastic material behavior (O'Dowd et al., 1992a). The load-deflection in cementitious interface system shows almost linear behavior up to failure point if the initial

nonlinear behavior due to machine setting is ignored (Fig. 3). Also, the inelastic zone of interface crack tip might be small enough to consider LEFM since there is no aggregate inter-locking or fiber bridging across the interface. Thus, a fully elastic calibration function can be used to interpret the interface fracture toughness.

For the bend geometry (Fig. 2),  $K$  is given by

$$K = YT\sqrt{aa^{-ie}} \exp(i\psi), \quad (10)$$

where  $a$  is the crack length (Huchinson et al., 1991). Eqn (10) is a specific form of Eqn (4) with  $L = a$ .

For the symmetric set-up, the nominal stress  $T$ , the 'geometric' and 'material' correction factor  $Y$ , and phase angle  $\psi$  are defined as

$$T = \frac{P}{t} \cdot \frac{3B}{2W^2}, \text{ and } Y = [f_1^2 + (2\epsilon g_2)^2]^{1/2} \text{ with } \psi = \tan^{-1}\left(\frac{2\epsilon g_2}{f_1}\right). \quad (11)$$

For the asymmetric set-up,  $T$ ,  $Y$  and  $\psi$  are defined as

$$T = \frac{P}{tW} \left[ \frac{B-A}{B+A} \right], \text{ and } Y = (Y_1^2 + Y_2^2)^{1/2} \text{ with } \psi = \tan^{-1}\left(\frac{Y_2}{Y_1}\right) \quad (12)$$

where

$$Y_1 = \frac{6s}{W} f_1 - 2\epsilon g_1, \quad Y_2 = f_2 + \frac{12s}{W} \epsilon g_2 \quad (13)$$

The calibration functions,  $f_1, f_2, g_1$  and  $g_2$ , have been determined numerically by O'Dowd et al. (1992a) as functions of  $(a/W)$ , and for different values of  $\alpha$  and  $\beta$ . Thus, the magnitude of interface toughness  $K_c$  and its phase angle are

$$K_c = YT_c \sqrt{a} \quad (14)$$

$$\hat{\psi} = \psi + \epsilon \ln(l/a)$$

Where  $T_c$  corresponds to the critical load at which the interface crack propagates. The calibration functions ( $f_1, f_2, g_1$  and  $g_2$ ) were interpolated values from "plot of calibration functions" (O'Dowd et al., 1992a) over a range of  $\alpha$  with  $\beta = \alpha/3$ . This value of  $\beta = \alpha/3$  is closest to the  $\beta = 3/8\alpha$  appropriate for the cementitious materials. However,  $f_1, f_2, g_1$  and  $g_2$  are not much different from those for

$\alpha = \beta = 0$  because  $\alpha$  and  $\beta$  are very small values for the repair systems in this test. Also, the somewhat arbitrary value  $200 \mu\text{m}$  is used for  $l$ . The phase angle changes only  $0.28^\circ$  for changing  $l = 200 \mu\text{m}$  to  $l = 2 \text{ mm}$  in concrete/concrete repair system.

The first peak load  $P_c$  of each test is used for the  $P$  in Eqn (11) and Eqn (12) to calculate  $T_c$ . Actual phase angles are calculated using  $s$ ,  $W$ ,  $\varepsilon$ ,  $l$ , the calibration functions, and the Young's moduli measured for each material. The resulting  $T_c$  and  $\psi$  are used to compute  $K_c$  and  $\hat{\psi}$  in Eqn (14). The  $K_c(\hat{\psi})$  is then reported as phase angle dependent interface toughness for each bimaterial system.

### 3.3 Materials

Three different repair materials were tested with substrate concrete. For the substrate concrete, 28 MPa compressive strength concrete at 7 weeks old including one week drying was used. For the repair material, the same concrete, FRC (1% volume fraction, ZL 30/50 hooked steel fiber), and FSHP (Five Star Highway Patch, a proprietary quick set concrete repair material on MDOT's qualified materials list) were used. The FSHP is specified to gain compressive strength 41.4 MPa at one day age. Table 1 contains the material mix proportions.

Table 2 contains information on the Young's modulus and elastic mismatch parameters for the three bimaterial systems tested. The elastic moduli were measured from compression test with two strain gages. The reported data represents the average of test results from three 7.62x15.24 cm (3x6 in.) cylinders. Substrate concrete was water cured for six weeks. Two week water curing was used for the repair materials.  $\alpha$ ,  $\beta$ , and  $\varepsilon$  are calculated from elastic moduli of materials

Table 1. Repair material mix design

Material	Cement	Water	FA	CA	Fiber <sup>†</sup>
Concrete	1.0	0.5	2.27	1.8	–
FRC	1.0	0.5	2.27	1.8	0.01
FSHP	1.0*	0.12	–	0.6	–

(FA: standard sand, CA: crushed stone ( $d < 9.5 \text{ mm}$ ), <sup>†</sup> volume fraction, \* the dry mix as received (cement+other materials) in FSHP)

Table 2. Interface systems and material parameters

Base Material	Repair Material	E1 (GPa)	E2 (GPa)	$\alpha$	$\beta$	$\varepsilon$
Concrete	Concrete	25.8	24.9	0.018	0.007	-0.0021
Concrete	FRC	25.8	26.1	-0.005	-0.002	0.0006
Concrete	FSHP	25.8	30.7	-0.087	-0.033	0.0104

(Eqn (1) and Eqn (2)) with  $\nu = 0.2$  assumed in all cases.

Twelve bimaterial beam specimens were cast for each repair material. All specimens were cured under the same curing condition. Substrate concrete beams were moisture cured for 24 hours before demolding, and cured in room temperature water for four weeks. Then, they were dried for a week before casting with repair materials, and cured two more weeks in room temperature water. All specimens were dried 24 hours before interface toughness testing. Thus, the substrate material cured 6 weeks in water, and the repair material cured 2 weeks in water.

### 3.4 Results of experiments

In most cases, the load–deflection curves show one steep load drop after first cracking, suggesting that the interface crack propagates rapidly once initiated, and completely ruptures the specimens. Fig. 3 shows the typical load–deflection relationship. Even though some test results show post peak behavior, the magnitude of the second or third peak load is usually negligible compared to the first.

Fig. 4, 5, and 6 plot the measured interface toughness  $K_c$  of three different interface systems with varied phase angles  $\hat{\psi}$  ranging from  $\sim 0^\circ$  to  $\sim 45^\circ$  (Table 3). The interface toughness of all three interface systems generally increases with increasing phase angle. Some specimens failed to generate toughness data at higher phase angle ( $>45^\circ$ ) since they broke in flexure away from the interface before the

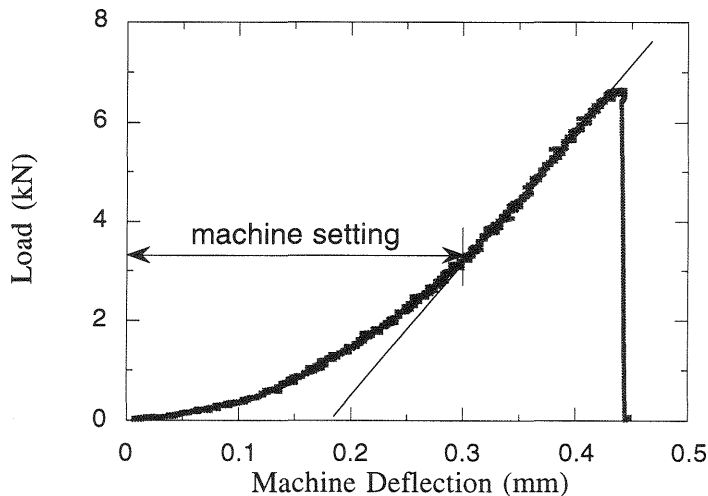


Fig. 3. Typical load–deflection relationship

interface crack propagates. The flexural failure occurs at the highest bending moment section (Fig. 2b).

The interface toughness of concrete-FRC interface system is slightly higher (about 18%) than the other two systems (Fig. 7). This trend is consistent with the bond strength measurement in carbon and steel micro fiber composites as a repair material (Banthia et al., 1994). A possible mechanism of this phenomenon suggested by Banthia et al. (1994) is that fibers reduce the size of flaws developed by shrinkage at the bimaterial interface.

In most cases, the interface crack clearly propagates along the interface with only small remnants of adjoining material remaining on the interface fracture surface. In other cases, especially at higher phase angle ( $>30^\circ$ ), the interface crack propagates along the interface for approximately 2/3 of the remaining beam depth, at which point the crack bifurcates and runs through the repair material. It may be an effect of stress field change as the interface crack approaches the upper beam surface near the load point, but the second load peak due to this bifurcation is negligible. On the other hand, several specimens of the concrete-FSHP interface system show kinking of the crack directly into the repair material from the notch tip rather than propagate through the interface, giving a lower bound for interface toughness (Fig. 6). These cases in the concrete-FSHP bimaterial system are also included in Table 3 as a lower bound of the system. It suggests that the relative toughness of the interface to that of the FSHP material is high enough to provide a favorable condition for kink-out as the phase angle increases.

The typical error bar represented in Fig. 4, 5, 6, and 7 contains the load-cell sensitivity ( $\pm 1\%$ ), the measuring errors of  $A, B$ , and  $s$  ( $\pm 0.3$  mm), and the variation of beam thickness ( $< 2\%$ ).

#### 4 Conclusion Remarks

In this study, interface toughness in different cementitious repair systems is experimentally measured. The measured interface toughness values were found to increase with increasing phase angle up to  $45^\circ$ . It is expected that still higher toughness will result if measured at higher phase angle. This increasing trend of phase angle dependence of interface toughness for cementitious material is consistent with other bimaterial system.

No significant difference is found among the different interface systems tested although the FRC repair material tends to give approximately 18% higher values than concrete repair material at all phase angles. The micromechanisms responsible for the increasing

trend of interface toughness vs. phase angle, and the higher toughness values for Concrete/FRC system are not at present understood.

The experimental program reported in this paper encounters a limitation. No interface toughness at phase angle higher than 45° was obtained. This limitation can be overcome with modification of specimen geometry to prevent flexural failure outside the interface.

In further studies, limited tests have been planned to verify that the measured interface toughness is independent of specimen size and geometry. Also, cementitious composites with pseudo strain hardening behavior will be used as a potential repair material.

Table 3. Experimental data of interface toughness tests

Materials	s (mm)	$\hat{\psi}$ (deg.)	$P_c$ (kN)	$K_c$ (MPa $\sqrt{m}$ )	$\Gamma$ (J/m <sup>2</sup> )	Failure Mode	
Concrete–Concrete	symm.	0.52	0.614	0.235	2.10	I	
		0.52	0.631	0.242	2.21	I	
		0.52	0.850	0.326	4.02	I	
	45	15.93	1.477	0.232	2.03	I	
		15.93	1.468	0.230	2.01	I	
	15	39.54	6.539	0.427	6.91	B	
		39.54	6.374	0.416	6.56	B	
		39.54	6.663	0.435	7.17	I	
	12	45.82	7.339	0.424	6.82	I	
	Concrete–FRC	symm.	-0.15	0.979	0.375	5.20	I
			-0.15	0.645	0.247	2.26	I
		45	15.11	2.887	0.451	7.53	I
15.11			1.300	0.203	1.52	I	
15.11			1.948	0.304	3.43	I	
20		31.42	5.587	0.439	7.12	I	
		31.42	4.337	0.341	4.29	I	
15		39.20	9.025	0.585	12.68	I	
		39.20	7.060	0.458	7.76	B	
12		45.57	9.029	>0.518	>9.95	F	
Concrete–FSHP		symm.	-2.58	0.566	0.217	1.61	I
			-2.58	0.549	0.210	1.51	I
	-2.58		0.710	0.272	2.53	I	
	45	12.90	1.835	0.283	2.71	I	
		12.90	1.789	0.276	2.60	I	
	20	29.84	3.395	0.260	2.32	I	
		29.84	5.729	0.439	6.60	K	
		29.84	4.303	0.330	3.73	I	
	17	34.36	7.360	0.504	8.68	I	
	15	38.01	6.650	>0.420	>6.04	K	
		38.01	5.810	>0.367	>4.61	K	
	12	44.73	9.400	>0.526	>9.46	F	

Failure Mode: I (interface cracking), B (interface cracking and kinking), F (flexural failure), K (kinking from notch tip)

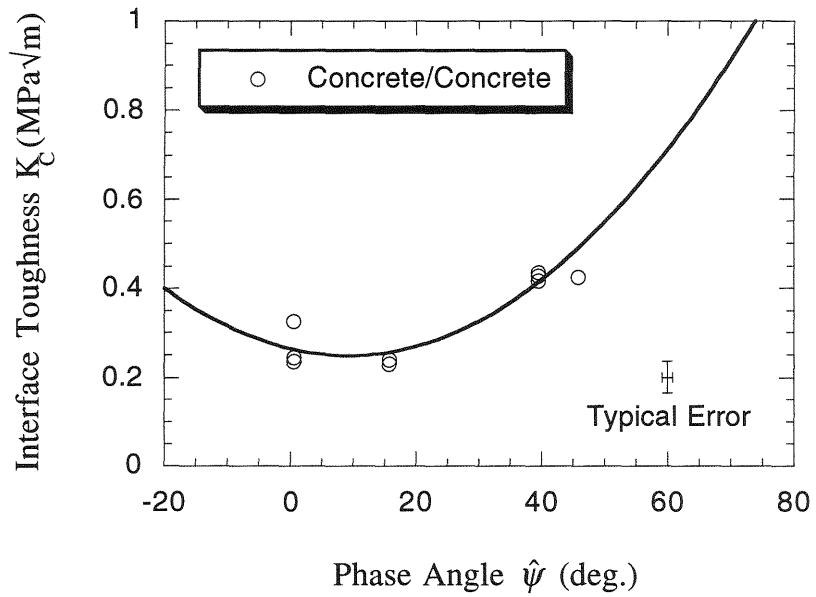


Fig. 4. Interface toughness in concrete–concrete interface system

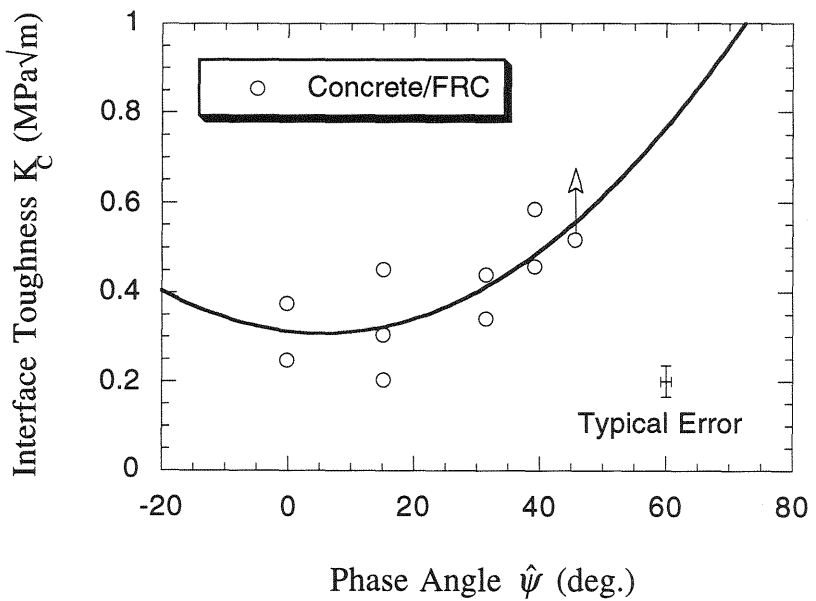


Fig. 5. Interface toughness in concrete–FRC interface system

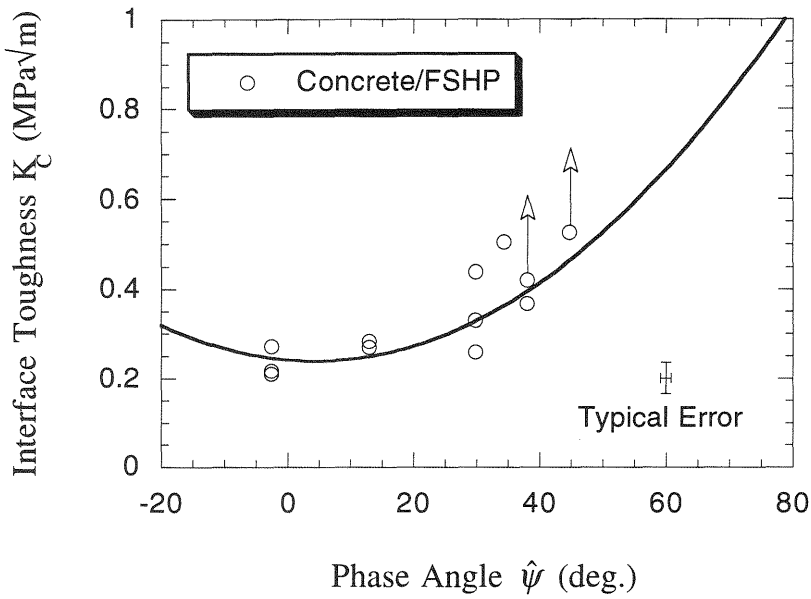


Fig. 6. Interface toughness in concrete–FSHP interface system

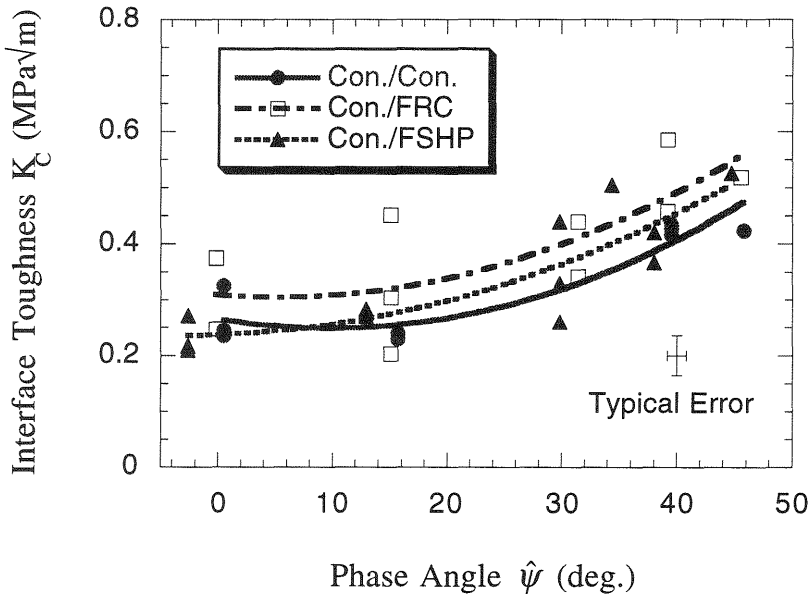


Fig. 7: Interface toughness for all bimaterial interface system tested

## 5 Acknowledgment

This work has been partially supported by a grant from the National Science Foundation to the University of Michigan. D.J. Foremsky's graduate study was supported by the Benton Fellowship. Useful discussions on interface mechanics with M. D. Thouless and on concrete repair with J. Warner are gratefully acknowledged. Also, thanks are due to D. Branch of MDOT for discussion relating to the repair of concrete and the evaluation of repair materials, and to J. Graveline of Five Star Products, Inc. for providing testing material and technical assistance.

## 6 References

- Allen, R.T.L., Edwards, S.C., and Shaw, J.D.N. (1993) **Repair of Concrete Structures**. 2nd ed., Chapman and Hall.
- Banthia, N, and Dubeau, S, (1994) Carbon and steel microfiber-reinforced cement-based composites for thin repair. **J. of Materials in Civil Engineering**. 6, No.1, 88–98.
- Buyukozturk, O., (1993) Interface Fracture and Crack Propagation in Concrete Composites, **Micromechanics of Concrete and Cementitious Composites**, (ed. by C. Huet) 203–212.
- Calvo, L. and Meyers, M. (1991) Overlay materials for bridge decks. **Concrete International**, July.
- Cao, H.C., and Evans, A.G. (1989) An experimental study of the fracture resistance of bimaterial interface. **Mechanics of Materials**. 7, 295–304.
- Charalambides, P.G., Lund, J., Evans, A.G., and McMeeking, R.M. (1989) A test specimen for determining the fracture resistance of bimaterial interfaces. **J. of Applied Mechanics**. 56, 77–82.
- Cherepanov, G.P. (1962) The stress state in a heterogeneous plate with slits. **Izvestia AN SSSR, ONT, Mekhan. i Mashin**, 1, 131–137.
- Emmons, P.H. (1994) **Concrete Repair and Maintenance Illustrated**. Construction Publishers & Consultants, Kingston.
- Elfgrén, Z. (1989) ed., **Fract. Mech. of Concrete Structures**. (Report of RILEM Techn. Committee TC 90–FMA), Chapman and Hall, London.
- England, A.H. (1965) A crack between dissimilar media. **J. Appl. Mech.** 32, 400–402.

- Erdogan, F. (1965) Stress distribution in bonded dissimilar materials with cracks. **J. Appl. Mech.**, 32, 403–410.
- He, M.Y., Bartlett, A., and Evans, A.G. (1991) Kinking of a crack out an interface: role of in-plane stress. **J. Am. Ceram. Soc.** 74, No. 4, 767–771.
- He, M.Y., and Hutchinson, J.W. (1989) Kinking of a crack out of an interface. **J. Appl. Mech.**, 56, 270–278.
- Huchinson, J.W. and Suo, Z, (1991) Mixed mode cracking layered materials. **Advances in Applied Mechanics.** 29.
- Jonston C.D., and Carter, P.D., (1989) Fiber reinforced concrete and shotcrete for repair and restoration of highway bridges in Alberta, in **International Symposium on Recent Developments in Concrete Fiber Composites.** Transportation Research Record 1226. 7–16.
- Liechti, K.M. and Chai, Y.–S. (1991) Biaxial loading experiments for determing fracture toughness. **J. Appl. Mech.** 58, 680–687.
- Mailvaganam, N.P. (1992) **Repair and Protection of Concrete Structures.** CRC Press.
- Malyshev, B.M., and Salanik, R.L. (1965) The strength of adhesive joints using the theory of cracks. **Int. J. Fracture Mech.**, 5, 114–128.
- O'Dowd, N.P., Shih, C.F., and Stout, M.G. (1992a) Test geometry for measuring interfacial fracture toughness. **Int. J. of Solids Structures.** 29, No. 5, 571–589.
- O'Dowd, N.P., Stout, M.G., and Shih, C.F. (1992b) Fracture toughness of alumina–niobium interface: experiments and analyses. **Philosophical Magazine A.** 66, No. 6, 1037–1064.
- Rice, J.R. and Sih, G.C. (1965) Plane problems of cracks in dissimilar media. **J. Appl. Mech.**, 32, 418–423.
- Rice, J.R. (1988) Elastic fracture concepts for interfacial cracks. **J. Appl. Mech.**, 55, 98–103.
- Wang, J.S., and Suo, Z. (1990) Experimental determination of interfacial toughness curves using Brazil–Nut–Sandwiches. **Acta metall. mater.** 38, No. 7, 1279–1290.
- Warner, J. (1994) Even with innovative materials, the basic still matter, in **Infrastructure: New Materials and Methods of Repair.** Proceedings of the Third Materials Engineering Conference (ed by K.D. Basham), ASCE, 72–79.